Chapter

Dynamic Effect in Fatigue on High-Deflection Structures

Raphael Paulino Goncalves

Abstract

There are a few kinds of structures that are created to fill in as a system, for example, springs, torsion bars, and axles, among others. They are structures, since they comprise of one single body, with no movement joints, however, with degrees of freedom, allowed by the mechanical compliance of the body. This aspect is extremely difficult to represent in durability assessment, since these structures-mechanisms are highly sensitive to dynamic effect of the system and the traditional method to predict fatigue (load history) is static and does not consider how the structure responds dynamically to the loading. In this chapter, we will study the fatigue behavior of two generic components, a classical structure and a structure-mechanism, using three different methods of calculation: load history (static), transient modal superposition (dynamic), and frequency domain modal superposition (dynamic). The objective is to demonstrate the differences between each calculation methodology due to the different ways each considers the dynamic effect.

Keywords: fatigue, structure, mechanism, deflection, dynamic, static, modal, superposition, transient, frequency, domain

1. Introduction

A mechanism is a system of multiple bodies assembled by one or many joints, with the objective to change a given input set of forces and moments to a desired output set of forces and moments. In a traditional mechanism, joints or kinematic pairs interface these bodies, giving relative movement between them. The combination between all bodies and joints produces the degrees of freedom of the component.

However, it is possible to design mechanisms with the desired degrees of freedom, without relying on joints and kinematic pairs. Compliant structures can produce relative movement depending on its design shape and the elastic characteristic of the material it consisted, by high mechanical strains.

A high mechanical strain implies that the absolute deflection of a body is "huge" when contrasted with its original form (without any deflection). Although there is no standard to characterize what is "huge," it is very much acknowledged and broadly received as strains higher than 5% [1].

However, even with "huge" strains, the material of the structure must always be inside the elastic region; otherwise, the mechanical work can cause failure. This can be achieved by tuning the design accordingly to the material used. For example, rubbers in simple prismatic rectangles can achieve "huge" deflections in axial directions, while steel must be in a different shape as a coil spring.

The utilization of components dependent on mechanical strain rather than kinematic sets is basic in the industry. Torsion axles, coil springs, leaf springs, and stabilizer bars are a few models broadly embraced in business applications, for example, trains, planes, and vehicles.

Due to its larger compliance and, therefore, natural degrees of freedom, the mechanism-structures respond differently to dynamic inputs, usually presenting lower natural modes. This characteristic has an important influence in fatigue performance when the loading input is dynamic.

To measure this influence, we will study in this chapter the fatigue performance using three different approaches: static load history, transient modal superposition, and frequency domain modal superposition.

2. Methods and materials

2.1 Dynamic and static loading

An important definition to establish is the difference between static and dynamic loading. In theory, a load is static when time is not considered at its application and, therefore, inertial reaction of bodies is not part of the calculation. In practice, pure static load does not exist, since the load will require an amount of time to be applied at a body. In physical environment, a load can be considered static when not producing relevant inertial effects to the system.

Figure 1 shows two beams with the same length and section. The beams are constrained at the left extremity and have an actuator applying force at the right extremity. The actuators are applying the same F force in both beams; however, the actuator on the left is applying the F force in a large amount of time, which is not enough to produce any relevant inertial effect to the system and therefore can be considered static. The actuator on the right is applying the F force but in a small amount of time, which creates relevant inertial effects to the system and therefore can be considered dynamic.

2.2 The chosen structures and the method for analysis

The structure-mechanism chosen for our study in this chapter is a torsion axle and the pure structure a sub-frame. Both are structures of the same system, a commercial vehicle. The system "vehicle" was chosen here for a reason, to submit the two structures to the same loading condition. The geometries in this chapter are simplified

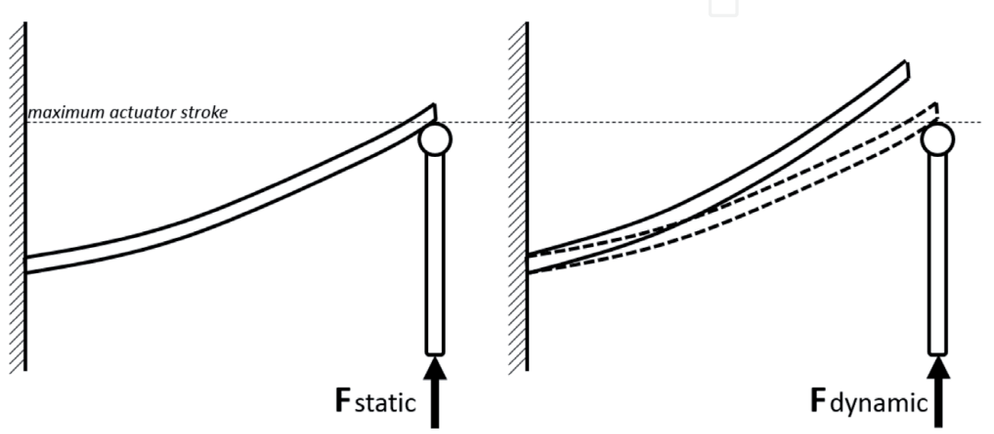

Figure 1.
Comparison between two beams under a force with the same magnitude but different duration of application.

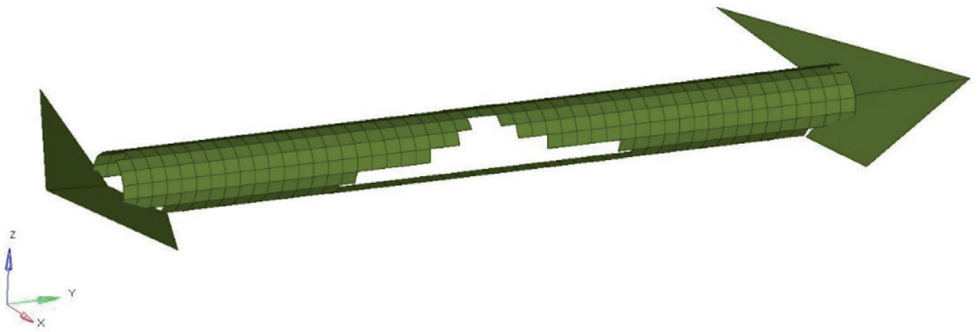

Figure 2.
Torsion axle—High displacement structure. The geometry was conceived using a topology optimization algorithm just for this study.

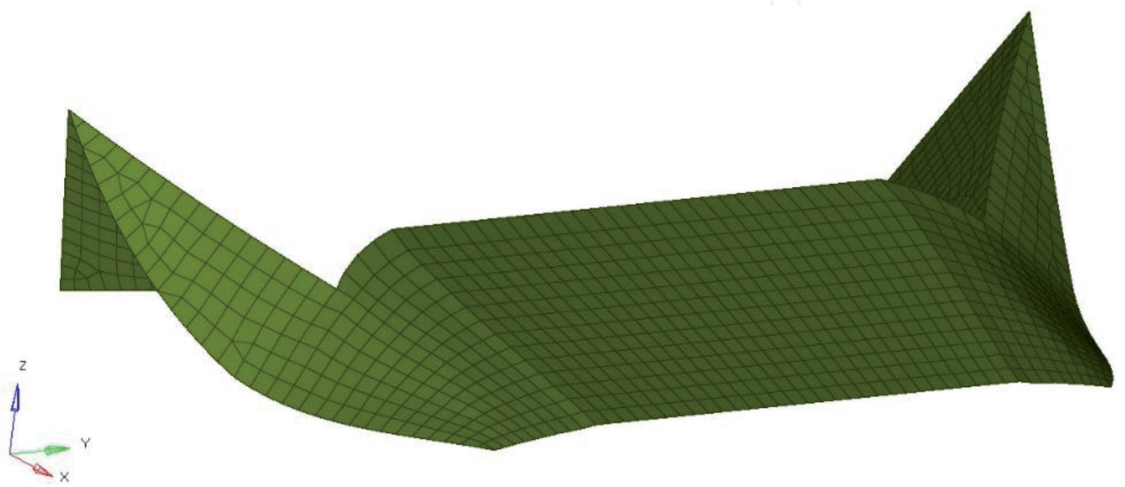

Figure 3.
Sub-frame—Pure structure. The geometry was also conceived using a topology optimization algorithm just for this study.

models created only for academic purposes, based on the same characteristics of the original models. They have the same mass, stiffness, and normal modes of the real torsion axle and sub-frame. The geometries were developed using topology optimization algorithms in order to maintain the same mentioned physical and mechanical properties. The models are conceived in finite element shell based (CQUAD4 elements) on structural analysis required in this chapter (stress/strain for fatigue and modal). The material considered for the structures is common steel, both with the same fatigue properties in order to make the comparisons of this study consistent (**Figure 2**).

The torsion axle is a common component present in commercial vehicles, used to support the entire suspension system (usually the rear suspension), since all suspension parts are attached to it, such as springs, shocks, and wheels. It performs also as a stabilizer beam, linking the left side to the right.

The sub-frame (**Figure 3**), also known as cradle, is a part of the vehicle used to attach the entire front suspension framework. It transmits all forces that came from the road from suspension to the body of the vehicle, and it has no relative movement between its points of interface. Uniquely in contrast to the torsion axle, it does not act as a stabilizer bar; in fact, in many vehicle designs, the sub-frame supports a stabilizer bar.

2.3 The load inputs

The loading conditions were obtained using a multi-body dynamic model (**Figure 4**) of the vehicle. This multi-body vehicle runs a rough road track made of Belgian blocks as the same way of a physical vehicle [2].

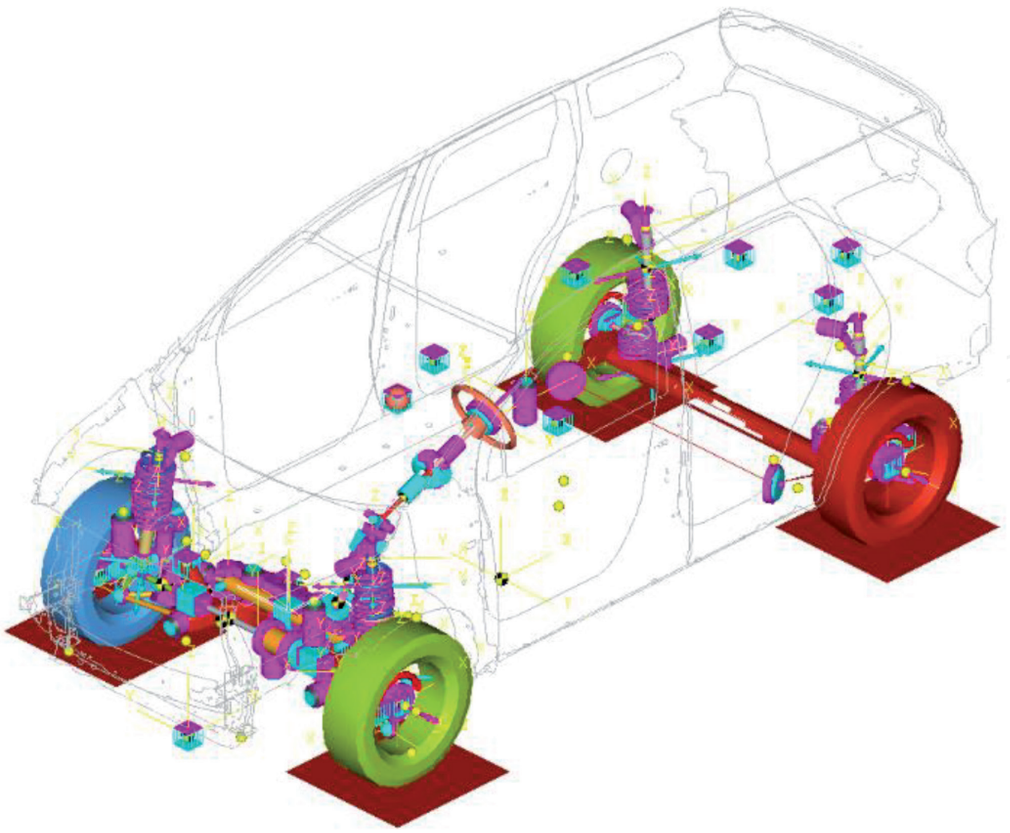

Figure 4.
Multi-body vehicle model used for loads acquisition.

The reason for using rough road Belgian blocks track is to submit both structures to a high-cycle fatigue, instead of a high-load low cycle. Also, this kind of track can produce dynamic loads as we already defined previously.

2.4 The dynamic effect

Before examining the durability behavior of the two structures, it is imperative to understand how they react dynamically to any set of loads. The study in this chapter proposes simply to contrast the distinctions of these two structures in a dynamic domain. For this reason, the modal analysis can, in a roundabout way, show how each structure reacts to dynamic conditions. The lower the mode, the

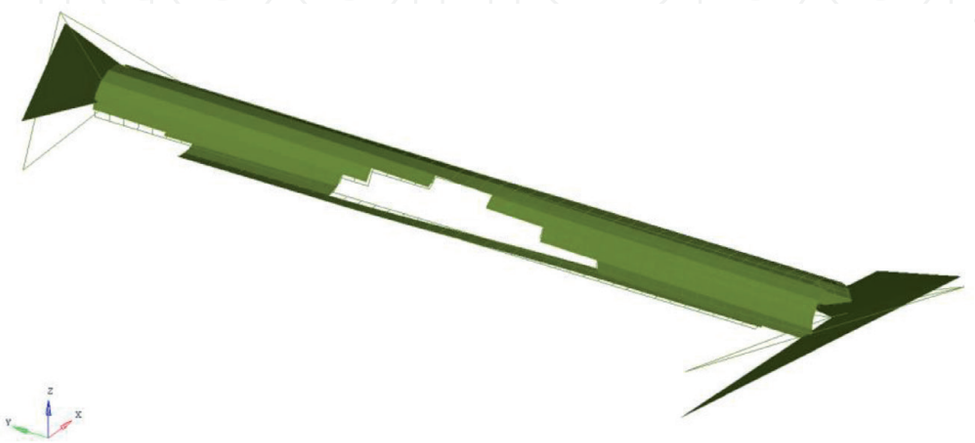

Figure 5.
Torsion axle: First normal mode of 33 Hz.

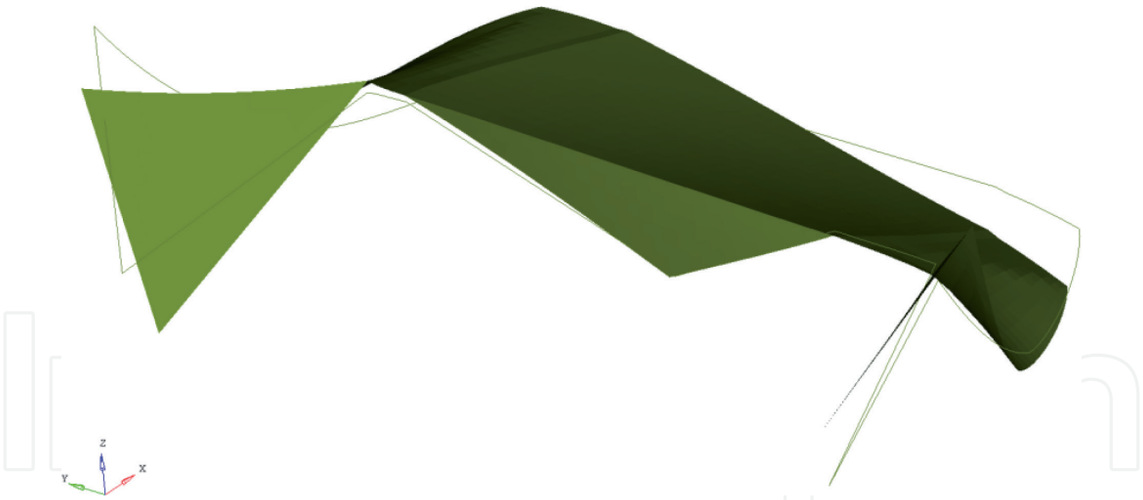

Figure 6.
Sub-frame: First normal mode of 283 Hz.

more probable the structure may enter in resonance during a given random load input. When this happens, the system starts to store kinetic energy and oscillate in a higher amplitude, affecting the durability performance.

The two structures presented in this chapter, the sub-frame (pure structure) and the torsion axle (mechanism-like structure), were submitted to a simple modal analysis using a standard commercial finite element analysis software. It is possible to see how each of them has different first natural modes (**Figure 5**).

Because of the lower compliance, the sub-frame has a higher first normal frequency than the torsion axle, 283 Hz (**Figure 6**) for the sub-frame and 33 Hz for the torsion axle. Until reaching the first normal frequency of the sub-frame (283 Hz), the torsion axle will have also other seven normal frequencies, representing seven different modes to resonate in a frequency sweep from 0 to 283 Hz, while the sub-frame will have only one mode.

2.5 Fatigue assessment

2.5.1 Process introduction

The fatigue assessment combines the stress/strain results with the repetitions from the event to calculate the damage/life. The stress/strain results in this chapter came from the finite element mode and the load magnitude, and repetitions came from the multi-body model running the Belgian block track.

2.5.2 Static load history approach

The durability analysis utilizing the load history approach is the less difficult and most customary method for computing fatigue of a given event. It is performed by applying a unitary static load to each interface point of the structure and after that, consolidating the results of stress/strain utilizing direct superposition (**Figure 7**).

The models are loaded with linear unit magnitude static loads (forces and moments) in each degree of freedom (6 in total), and the result is the elemental stress.

These stresses are then used by the fatigue solver. The elemental stress result is combined to calculate the fatigue damage of the event, in this case, the Belgian blocks.

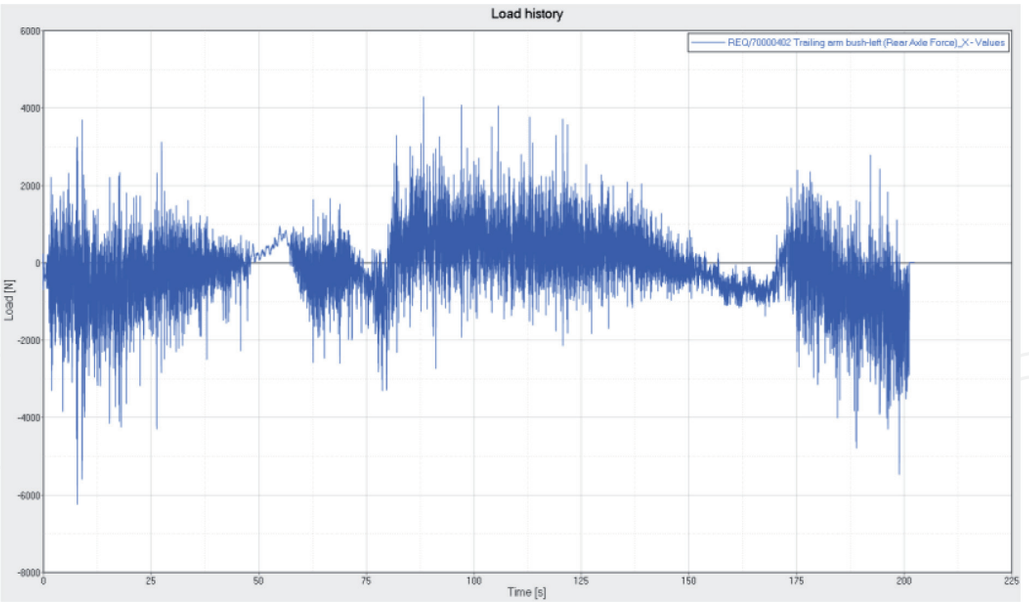

Figure 7.
Load history (load × time) of one hard point of the torsion axle in the X-axis.

2.5.3 Transient and frequency domain modal superposition

The equation for dynamic motion of a system with linear single degree of freedom is given by the following:

$$M_{mass}\frac{\partial^2 x}{\partial t^2}(t) + C_{damping}\frac{\partial x}{\partial t}(t) + K_{stiffness}x(t) = L_{load}(t) \tag{1}$$

The output of the system is a rotation or displacement, in function of a time t. Eq. (1) is a second-order ordinary differential equation that can describe the motion of the system, by its acceleration (second derivative of displacement in respect of time), velocity (derivative of displacement in respect of time), and displacement.

The Duhamel integral can provide a solution for a given $L_{load}(t)$ for any instant greater than zero, i.e.,

$$x(t) = \int_0^t L_{load}(t)h(t-\tau)d\tau \tag{2}$$

Equation (2) can be rewritten, considering that $h(t)$ is the unit impulse (Dirac's delta) response function.

$$x(t) = L_{load}(t) * h(t) \tag{3}$$

Equation (2) will only have solutions in very simple systems. In general conditions, Eq. (2) will only have solutions when using algorithms to perform numerical integrations. These solutions for Eq. (2) should introduce a few volatilities that force the utilization of little steps of time (t). Moreover, the procedure can have a high cost (computational) regarding handling a large amount of time fractions (since the time step is small, a larger number of time fractions will be needed to represent the entire event). For this, two fundamental arrangements are known in general as modal transient response and direct transient response.

On the other hand, by taking the Fourier transform of Eq. (3) and using the concepts of spectral analysis [3–10], it is possible to simplify the time involution integration by multiplying in time domain, i.e.,

taking the Fourier transform of Eq. (3) permits simplifying the solution of the time convolution integration in a simple multiplication in frequency (ω) domain, i.e.,

$$X(\omega_{frequency}) = P(\omega_{frequency})H(\omega_{frequency}) \tag{4}$$

Here, the functions $L_{load}(t)$, $x(t)$, $h(t)$ are replaced by its Fourier transform pair, i.e., if considering $x(t)$,

$$X(\omega_{frequency}) = \frac{1}{2\pi}\int_{-\infty}^{\infty} x(t)\, e^{-i\omega_{frequency}t}\, dt \tag{5}$$

$$x(t) = \int_{-\infty}^{\infty} X(\omega_{frequency})\, e^{i\omega_{frequency}t}\, d\,\omega_{frequency} \tag{6}$$

Here, $\omega_{frequency} = 2\pi f$, where $\omega_{frequency}$ and f are the linear and circular frequency variables, expressed, respectively, in [Hz] and [rad/s].

The last equation, Eq. (6), an inverse Fourier transform, and the normal Fourier transform in Eq. (5) can be numerically evaluated using FFT algorithms (fast Fourier transform) which are well-known and widely used.

The Fourier integrals in Eqs. (6), (5) will be valid, depending on the properties of the function considered. This occurs when the system in Eq. (1) is submitted to random loading inputs.

In the context of processes theory [2, 11–13], Eq. (4) must be used to handle input/output relationships when the system is submitted to random excitations.

A random event can be portrayed in frequency domain using spectral density functions. These functions, also known as power spectral densities (PSDs), along with the correlation functions are related by Fourier transform pairs.

The spectral density function $S_{xx}(\omega)$, for any stationary and ergodic random variable$x(t)$, is given by

$$S_{xx}(\omega_{frequency}) = \frac{1}{2\pi}\int_{-\infty}^{\infty} R_{xx}(t)\, e^{-i\omega_{frequency}\tau}\, d\tau \tag{7}$$

with

$$R_{xx}(\tau) = \int_{-\infty}^{\infty} S_x(\omega_{frequency})\, e^{i\omega_{frequency}\tau}\, d\omega \tag{8}$$

where $R_{xx}(\tau)$ is the autocorrelation of$x(t)$, or in other words, it is the expected value $E[x(t)x(t+\tau)]$, i.e.,

$$R_{xx}(\tau) = \lim_{T\to\infty}\frac{1}{T}\int_0^T x(t)x(t+\tau)dt \tag{9}$$

and, Fourier transform is valid to be applied over $R_{xx}(\tau)$, in certain conditions.

Equation (1) can be rewritten in form of a matrix for multiple degrees of freedom (MDOF), i.e.,

$$[M_{mass}]\left\{\frac{\partial^2 x}{\partial t^2}(t)\right\} + [C_{damping}]\left\{\frac{\partial x}{\partial t}(t)\right\} + [K_{stiffness}]\{x(t)\} = \{L_{load}(t)\} \tag{10}$$

The multiple load input spectral density also can be expressed in a matrix form given by (where m is the number of load inputs)

$$\left[S_{pp}(\omega_{frequency})\right]_{m\times m} = \begin{bmatrix} S_{11}(\omega_{frequency}) & \cdots & S_{1m}(\omega_{frequency}) \\ \vdots & \ddots & \vdots \\ S_{m1}(\omega_{frequency}) & \cdots & S_{mm}(\omega_{frequency}) \end{bmatrix} \tag{11}$$

where the off-diagonal terms $S_{ij}(\omega_{frequency})$ are the spectral densities for the cross-correlation of the load inputs ($L_{load_i}(t)$ and $L_{load_j}(t)$) and the diagonal term $S_{ii}(\omega_{frequency})$ is the auto spectral density of $L_{load_i}(t)$.

Therefore, in the frequency domain, the input/output relation for the matrix system in Eq. (10) is (where n is the number of output response variables)

$$\left[S||xx(\omega_{frequency})\right]_{n\times n} = \left[H(\omega_{frequency})\right]_{n\times m}\left[S_{pp}(\omega_{frequency})\right]_{m\times m}\left[H(\omega_{frequency})\right]^{T}_{m\times n} \quad (12)$$

The "*" is the complex conjugate and T denotes transpose matrix.

The matrix $\left[H(\omega_{frequency})\right]$ is the transfer function matrix between the input loads and output response variables, i.e.,

$$\left[H(\omega_{frequency})\right] = \frac{1}{-[M]\,\omega_{frequency}^{2} + i[C]\,\omega_{frequency} + [K]} \quad (13)$$

that can be calculated by standard FE solutions, as a unit modal frequency response. This transfer function becomes an input to the fatigue solver in frequency domain analysis process.

2.5.4 Conversion of loads from time to frequency domain

The loads needed for the frequency domain analysis must be created using a Fourier transformation. Customarily, the correct interpretation of the frequency domain approach depends upon three premises (stationarity, Gaussian, random) completely met. In any case, some flexibility is conceivable. Besides, there are methodology that can be applied to break down nonstationary (and nonrandom, non-Gaussian) data into shorter subcases that do conform in an adequate manner.

The loading channels on both strictures are comprised of the number of hard points (where the structure interfaces with the environment, like constrains and load inputs) times the degrees of freedom. The torsion axle for example has 48 loading channels, 8 hard points (as can be seen in **Figure 8**, hard points are represented as yellow circles) times 6 degrees of freedom. For the frequency domain approach to deal with the correlation between channels, the purported cross-PSD's are additionally required. Each channel requires a real and imaginary PSD (together they compose the complex cross-PSD), and these are observed in **Figure 9**.

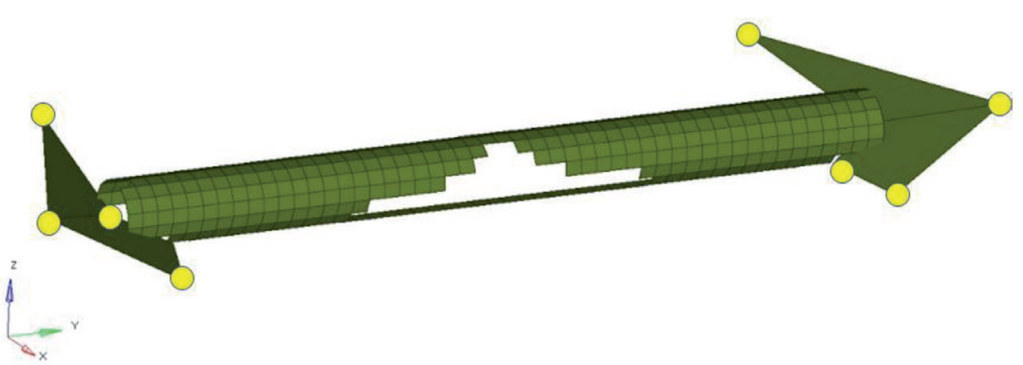

Figure 8.
The hard points of the torsion axle.

	channel 1	channel 2	channel 3	channel 4	channel 5	channel 6	...	...	...	...	...	...	channel 48
channel 1	PSD_1-1	PSD_1-2	PSD_1-3	PSD_1-4	PSD_1-5	PSD_1-6	PSD_1-7	PSD_1-8	PSD_1-9	...	...	...	PSD_1-48
channel 2	PSD_2-1	PSD_2-2	PSD_2-3	PSD_2-4	PSD_2-5	PSD_2-6	PSD_2-7	PSD_2-8	PSD_2-9	...	...	...	PSD_2-48
channel 3	PSD_3-1	PSD_3-2	PSD_3-3	PSD_3-4	PSD_3-5	PSD_3-6	PSD_3-7	PSD_3-8	PSD_3-9	...	...	...	PSD_3-48
channel 4	PSD_4-1	PSD_4-2	PSD_4-3	PSD_4-4	PSD_4-5	PSD_4-6	PSD_4-7	PSD_4-8	PSD_4-9	...	...	...	PSD_4-48
channel 5	PSD_5-1	PSD_5-2	PSD_5-3	PSD_5-4	PSD_5-5	PSD_5-6	PSD_5-7	PSD_5-8	PSD_5-9	...	...	...	PSD_5-48
channel 6	PSD_6-1	PSD_6-2	PSD_6-3	PSD_6-4	PSD_6-5	PSD_6-6	PSD_6-7	PSD_6-8	PSD_6-9	...	...	...	PSD_6-48
channel 7	PSD_7-1	PSD_7-2	PSD_7-3	PSD_7-4	PSD_7-5	PSD_7-6	PSD_7-7	PSD_7-8	PSD_7-9	...	...	...	PSD_7-48
channel 8	PSD_8-1	PSD_8-2	PSD_8-3	PSD_8-4	PSD_8-5	PSD_8-6	PSD_8-7	PSD_8-8	PSD_8-9	...	...	...	PSD_8-48
channel 9	PSD_9-1	PSD_9-2	PSD_9-3	PSD_9-4	PSD_9-5	PSD_9-6	PSD_9-7	PSD_9-8	PSD_9-9	...	...	...	PSD_9-48
...	...	...	...	...	...	...	...	...	...	...	...	...	...
...	...	...	...	...	...	...	...	...	...	...	...	...	...
...	...	...	...	...	...	...	...	...	...	...	...	...	...
channel 48	PSD_48-1	PSD_1-1	PSD_1-1	PSD_1-1	PSD_1-1	PSD_1-1	...	...	...	...	...	...	PSD_48-48

Figure 9.
Torsion axle. PSD matrix for event 1.

3. Results

As can be observed in durability results plotted (damage) on the sub-frame, the performances were practically indistinguishable among the three techniques. Because of the low compliance of the structure, the dynamic impact of the loading input is low, and accordingly, all techniques merged to an akin answer, as far as damage magnitude, yet additionally, damaged regions.

For the torsion axle, there was a bigger contrast, because of the dynamic influence. Its mechanism-like characteristic has a higher structural compliance, presenting higher deflections and relative movements between the interface points when submitted to loading. Also, its lower stiffness properties induce it to be more susceptible to dynamic influence as already explained. Due to that, a contrast between the static and dynamic durability assessment can be observed. It is usually hard to decide the significance of variations in fatigue results, for instance, if we accept we are managing a material that has a correspondent stress/strain-life slant of around 10, then we can convert the life or damage differences into stress/strain difference. In other words, we can assume the following relationship:

Damage variation = (damage to be compared/damage baseline)^.1

For instance, for the torsion axle, the static damage result is 38, and transient in frequency domain is 68, and in transient time domain is 198. If we consider the static as a baseline (since it is the lowest value), we can expect the following damage variation: 6% increase of damage for transient frequency domain and 11% increase of damage for transient time domain when compared to static.

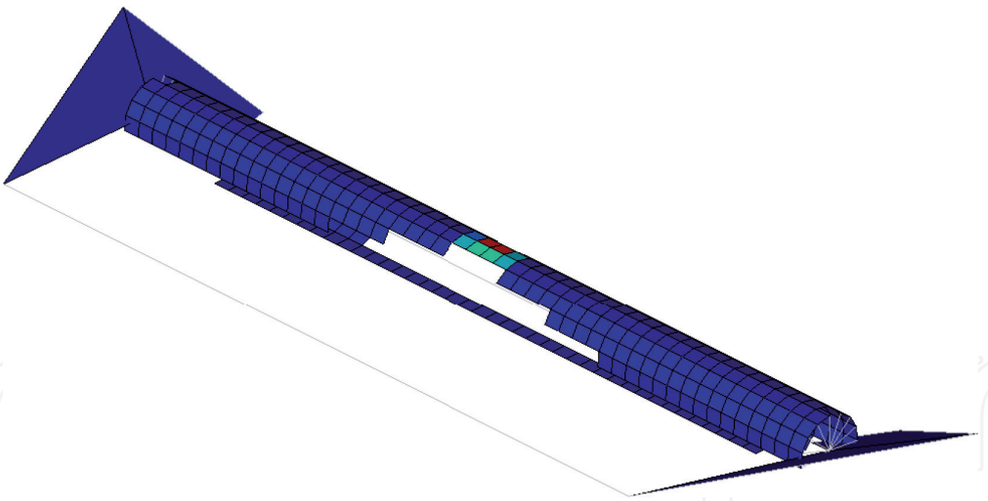

Figure 10.
Static load history damage result plot. Maximum damage = 38.

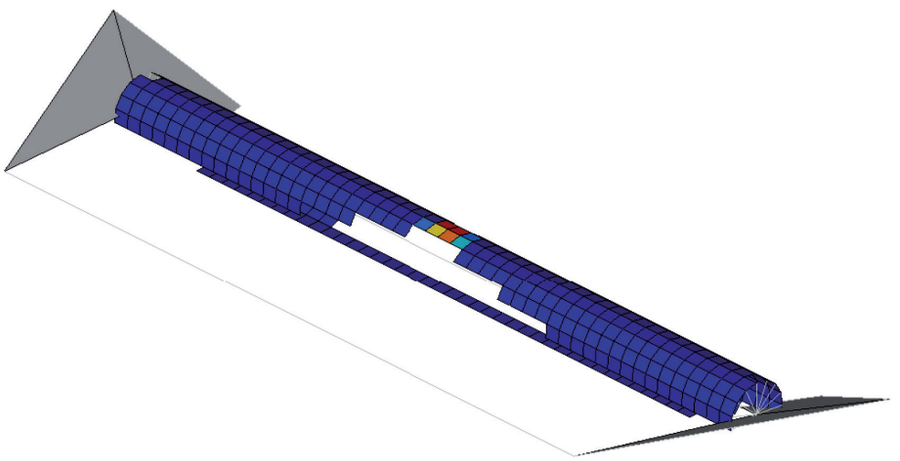

Figure 11.
Time domain modal superposition damage result plot. Maximum damage = 198.

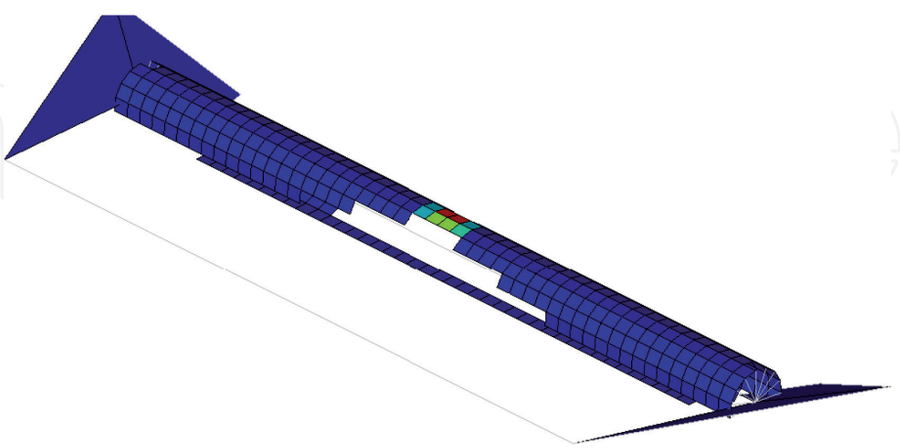

Figure 12.
Frequency domain modal superposition damage result plot. Maximum damage = 68.

When calculating damage using the static method, the dynamic effects are not considered, and accordingly, the result is the lowest among the other methods introduced. The transient method in time domain shows the higher damage.

Figure 13.
Static load history damage result plot. Maximum damage = 119.

Figure 14.
Time domain modal superposition damage result plot. Maximum damage = 116.

Figure 15.
Frequency domain modal superposition damage result plot. Maximum damage = 92.

The most damaged regions are also different among the three approaches on the torsion axle. It is possible to observe that the center was the most damaged region in all methodologies; however, the most critical elements are different. This suggests that these various approaches can point various conclusions as far as magnitude as well as most damaged regions (**Figures 10–15**).

4. Discussion

This chapter does not propose to conclude which methodology is the best. The static approach is the easiest method to numerically foresee the durability of a model; if the loading history is simple (cyclic with frequency below the first natural mode) or the structure is stiff (non-compliant, like the sub-frame), the static technique can achieve results with a similar quality as the two other dynamic approaches. But, if the loading history is complex (random, like the one utilized in this examination) or the structure is compliant (like the torsion axle), the static approach may not be enough to correctly calculate the durability of the structure, since it does not consider the dynamic effects.

However, during the development of any structure, it is common to find scenarios where it is difficult to determine if a signal is simple enough or a structure is stiff enough to relay only to the static methodology. In this chapter, the structures adopted as examples were previously known how to behave, but this may not be the case in most practical applications, since there is no formula or rule to guarantee the use of a specific approach. A modal analysis of the structure and a deep analysis of the signal may help to point a direction of which methodology to choose, static or dynamic, but still cannot conclude by its own.

When comparing the two dynamic methods, the transient modal superposition approach gave more conservative results in the example presented in this chapter. However, the underlying change in stress to cause the contrast is only 11%, and this could be by statistical scatter in the underlying random process. In this way, it is not conclusive which approach is more appropriate for this sort of structure. It has been reported that the frequency domain approach can be performed with considerably less computational resources and so could be preferred for large models [14].

Author details

Raphael Paulino Goncalves
General Motors, São Caetano do Sul, Brazil

*Address all correspondence to: raphael.p.goncalves@gmail.com

References

[1] Altair University, Introduction to Nonlinear Finite Element Analysis using OptiStruct, Altair; 2018

[2] Zhang Y, Stawiarski T, Subramanian M, Yung D, Farahani AD, Zhang X. Full Vehicle Finite Element Model 4-Post Durability Analysis. SAE Technical Paper 2005-01-1402. General Motors Corporation, Engineering Technology Associates, Inc. 2005. https://www.sae.org/publications/technical-papers/content/2005-01-1402/

[3] Leistein P. Frequency Domain Fatigue Analysis of Exhaust Systems. SAE; 2018

[4] Thesing T, Bishop N. Modern Methods for Random Fatigue of Automotive Parts. SAE Technical Paper 2016-01-0372; Hella KGaA Hueck and Co., CAEfatigue, Ltd; 2016. DOI: 10.4271/2016-01-0372

[5] Newland D. An Introduction to Random Vibrations, Spectral & Wavelet Analysis. 3rd ed. Dover Publications; 2005

[6] Maymon G. Structural Dynamics and Probabilistic Analysis for Engineers. Butterworth-Heinemann; 2008

[7] Karadeniz H. Stochastic Analysis of Offshore Steel Structures. Springer Series in Reliability Engineering. London: Springer-Verlag; 2013

[8] Ferreira W, Meehan T, Cardoso V, Bishop N. Comparative Study of Automotive System Fatigue Models Processed in the Time and Frequency Domain. SAE Technical Paper 2016-01-0377. Ford Motor Company, Valdirm Cardoso, CAEfatigue, Ltd.; 2016. https://doi.org/10.4271/2016-01-0377

[9] Bishop, Neil WM, Sherratt F. Finite Element Based Fatigue Calculations. Glasgow: NAFEMS Ltd; 2000

[10] Bishop N, Murthy P, Sweitzer K, Kerr S. Time vs Frequency Domain Analysis For Large Automotive Systems. SAE Technical Paper 2015-01-0535. Booz Allen Hamilton Inc., CAEfatigue, Ltd; 2016. DOI: 10.4271/2015-01-0535

[11] Bishop NSF. Fatigue life prediction from power spectral density data. Part 1, traditional approaches and part 2, recent developments. Env. Eng. 1989;**2**:2-11

[12] Bishop N, Kerr S, Murthy P, Sweitzer K. Advances Relating to Fatigue Calculations for Combined Random and Deterministic Loads. SAE International Paper 2014-01-0725; 2014. https://doi.org/10.4271/2014-01-0725

[13] Bishop N, Kerr S, Murthy P, Sweitzer K. Advances relating to fatigue calculations for combined random and deterministic loads. In: 13th International ASTM/ESIS Symposium on Fatigue and Fracture Mechanics (39th National Symposium on Fatigue and Fracture Mechanics). Jacksonville; 2013

[14] CAEfatigue VIBRATION (CFV) User Guide & Verification Manual (Release 3.0), UK: CAEfatigue Limited; 2016